

Urban aerosols and their variations with clouds and rainfall: A case study for New York and Houston

Menglin Jin

Department of Meteorology, University of Maryland, College Park, Maryland, USA

J. Marshall Shepherd

Laboratory for Atmospheres, NASA Goddard Space Flight Center, Greenbelt, Maryland, USA

Michael D. King

Earth Sciences Directorate, NASA Goddard Space Flight Center, Greenbelt, Maryland, USA

Received 1 June 2004; revised 26 January 2005; accepted 2 March 2005; published 27 April 2005.

[1] Diurnal, weekly, seasonal, and interannual variations of urban aerosols were analyzed with an emphasis on summer months using 4 years of the NASA Earth Observing System (EOS) Moderate Resolution Imaging Spectroradiometer (MODIS) observations, in situ Aerosol Robotic Network (AERONET) observations, and in situ U.S. Environmental Protection Agency (EPA) PM_{2.5} data for one midlatitude city (New York) and one subtropical city (Houston). Seasonality is evident in aerosol optical thickness measurements, with a minimum in January and a maximum in April to July. The diurnal variations of aerosols, however, are detectable but largely affected by local and regional weather conditions, such as surface and upper-level winds. On calm clear days, aerosols peak during the two rush hours in the morning and evening. Furthermore, the anthropogenic-induced weekly cycles of aerosols and clouds are analyzed, which by themselves are weak, as the anthropogenic signal is mixed with noise of natural weather variability. In addition, corresponding cloud properties observed from MODIS demonstrate an opposite phase to the seasonality of aerosols. Nevertheless, no clear relationship was observed between monthly mean aerosols and rainfall measurements from NASA's Tropical Rainfall Measuring Mission (TRMM), implying that in the summer the aerosol impact may not be the primary reason for the change of urban rainfall amount.

Citation: Jin, M., J. M. Shepherd, and M. D. King (2005), Urban aerosols and their variations with clouds and rainfall: A case study for New York and Houston, *J. Geophys. Res.*, 110, D10S20, doi:10.1029/2004JD005081.

1. Introduction

[2] The most recent *Intergovernmental Panel on Climate Change (IPCC)* [2001] report suggests that human activities are responsible for most of the warming observed in the past 50 years. Although IPCC has an emphasis on greenhouse warming, urban-induced surface warming (urban heat island effect (UHI)) and urban pollution impacts on surface energy budget have raised great concerns [Changnon, 1992; Grimmond and Oke, 1995; Arnfield, 2003; IPCC, 2001; Jin et al., 2005; Shepherd and Jin, 2004]. Urban areas, with rapid land cover and land use changes, suffer significantly from human activities. Understanding the human impacts on nature is a central component of global change studies. In addition, simulating urban environments in a climate model framework is a practical research approach [Jin and Shepherd, 2005].

[3] Aerosols and their relationships with clouds and rainfall are one of the weakest aspects of current climate modeling [Ghan et al., 2001]. Two limitations exist in current

urban modeling: (1) the aerosol effects on land surface skin temperature (namely, UHI) are either not included or unrealistically represented and (2) cloud-aerosol-rainfall relationships are not fully understood. (Land surface skin temperature is the radiometric temperature retrieved from satellite remote sensing based on the Planck function. This variable is a counterpart of the traditional WMO station measured 2 m surface air temperature, but is more close to the surface energy balance. It has been used to study global climate change. Atmosphere conditions such as clouds and aerosols have significant influences on skin temperature [Jin and Dickinson, 1999, 2000, 2002; Jin, 2000, 2004]). Previous results, via different approaches, have been controversial. For example, some studies reported that urban areas reduce rainfall due to cloud microphysics [Ramanathan et al., 2001], while other studies showed that urban areas significantly enhanced the intensity of storms and increased downwind rainfall [Huff and Vogel, 1978; Changnon, 1978; Shepherd et al., 2002].

[4] Better quantitative understanding of the spatial and temporal aerosol properties is desired in order to include urban aerosol radiative forcing and aerosol-cloud interactions

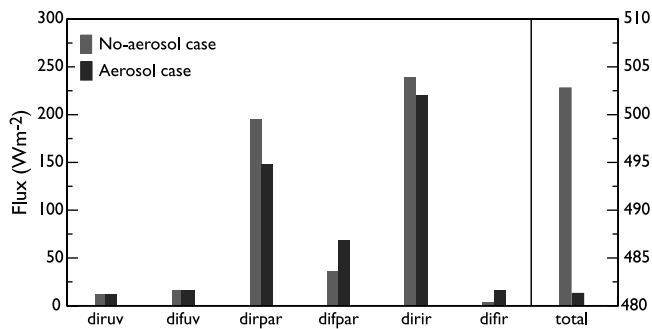


Figure 1. Changes of surface solar radiation induced by urban aerosols for 1 September 2001 based on simulations from a radiative transfer model developed by *Chou and Suarez* [1999]. Here “diruv” and “difuv” represent direct and diffuse UV radiation, “dirpar” and “difpar” represent direct and diffuse photosynthetically active radiation, and “dirir” and “difir” represent direct and diffuse near-infrared radiation. The “total” represents the total solar radiation, and the values are shown on the right-hand axis in Wm^{-2} .

in a general circulation model (GCM). Furthermore, observed climatological relationships between aerosols, clouds, and rainfall are needed for validating the modeled patterns in urban areas. This paper aims to describe the temporal variations of aerosols and to identify monthly mean aerosol-cloud-rainfall relationships from various remote sensing and ground-based measurements. Specifically, diurnal, weekly, seasonal, and interannual variations of urban aerosols are examined using 4 years of aerosol, cloud, rainfall, and land cover (namely, normalized difference vegetation index, NDVI) measurements from satellites. To demonstrate the similarities and differences of urban aerosols in different climate regions, we emphasize one midlatitude city (New York) and one subtropical city (Houston). In addition, the large-scale variables (wind and surface pressure) from the National Centers for Environmental Prediction (NCEP) reanalysis reveal how the atmospheric system controls the transport of urban aerosols.

[5] Aerosol radiative forcing, the so-called “direct effect,” means that aerosols reduce surface insolation by scattering and absorbing solar radiation and reemitting long-wave radiation back to the surface [*Ramanathan et al.*, 2001]. In addition, aerosols affect the climate system through aerosol-cloud interactions, primarily in three ways: (1) aerosols reduce the cloud effective radius and increase the cloud optical thickness as cloud condensation nuclei (CCN) increase, namely, the “indirect effect” [*Twomey*, 1977; *King et al.*, 1993]; (2) aerosol heating changes atmosphere stability and thus the occurrence and evaporation of clouds (“semi-indirect effect”) [*Hansen et al.*, 1997]; and (3) clouds affect aerosol properties. For example, it was reported that the cloud diurnal cycle affects aerosol forcing over the Indian Ocean Experiment up to $1\text{--}2 \text{ Wm}^{-2}$. Similarly, aerosol size distribution can be changed due to aerosol-cloud interactions [*Remer and Kaufman*, 1998].

[6] Produced by combustion of fossil fuels from traffic or industrial processes and modified through chemical composition, decomposition, and transport, urban aerosols are directly related to human activities and are gaining increasing

attention [*IPCC*, 2001; *Lelieveld et al.*, 2001; *Ramanathan et al.*, 2001; *Kaufman et al.*, 2002]. Figure 1 shows the simulated aerosol-induced changes in surface insolation based on the AERONET-observed aerosol optical properties for New York on one day in September (1 September 2001). The total reduction in insolation for this day is about 20 Wm^{-2} , with the maximum reduction in the photosynthetically active radiation (PAR) region of the solar spectrum between clean and polluted cases. The calculation uses the NASA Global Modeling and Assimilation Office’s (GMAO’s) GCM radiative transfer scheme [*Chou and Suarez*, 1999]. The model requires input of aerosol optical thickness, single scattering albedo, asymmetry factor, vertical aerosol distribution, and cloud cover. Obviously, these properties of urban aerosols vary spatially and temporally and are required in aerosol impact studies.

[7] Spectral aerosol optical thickness (AOT) represents the attenuation of sunlight by a column of aerosols at certain wavelengths, and has been used to assess aerosol condensation [*Kaufman et al.*, 2002]. Therefore AOT is the key parameter for modeling the radiative effects of aerosols in atmosphere columns, and is determined by the MODIS remote sensing algorithm [*Kaufman et al.*, 1997; *Chu et al.*, 2002, 2003]. In this paper, we study the optical thickness of aerosols and clouds to reveal their relationships. Furthermore, urban aerosols enhance aerosol-cloud interaction, which is expected to be more significant during the summer months when large-scale dynamical impacts are relatively weak in comparison to winter months. Therefore we emphasize the summer seasons for years 2000–2004.

[8] Scale is critical in urban studies, as urban features vary dramatically along both horizontal and temporal dimensions [*Oke*, 1982; *Jin et al.*, 2005]. We analyzed cloud-rainfall-aerosol relationships at monthly instead of daily scales, in particular, because we intended to identify the typical, climatological sense of aerosol properties and their effects on clouds and rainfall, and partly because the daily variations are more affected by white noise from surface and atmospheric conditions than the longer scales, and thus are not the major focus of this study.

[9] There are two foci in this paper. One is urban aerosols’ temporal variability (diurnal, weekly, seasonal, and interannual variations). Such knowledge is needed to accurately parameterize aerosol physical and chemical processes in a climate model. Another focus is the correlations among aerosols, clouds, and rainfall. Instead of studying cloud microphysics, we compared monthly variations to reveal the possibly existing climatological relationships of these variables. These observed features are very useful in validating model performance.

[10] The second section describes the data sets used in this work. The third section presents the results, and is followed by social, land cover, and general circulation backgrounds for New York and Houston that may shed light on explaining the differences in the aerosol properties for these two cities. Final remarks are presented in section 5.

2. Data Sets

2.1. MODIS Aerosol and Cloud Products

[11] Terra/MODIS monitors the aerosol optical thickness over the globe from a 705 km polar-orbiting Sun-synchro-

nous orbit that descends from north to south, crossing the equator at 1030 LT. The aerosol optical thickness (τ_a) over land is retrieved at 0.47, 0.56 and 0.65 μm and at a 10 km spatial resolution using the algorithm described by *Kaufman et al.* [1997]. The spectral dependence of the reflectance across the visible wavelengths is then used to obtain a rough estimate of the fine mode (radius $< 0.6 \mu\text{m}$) fraction of the aerosol optical thickness at 0.56 μm . The cloud optical thickness (τ_c) and effective radius (r_c) are retrieved at 1 km spatial resolution using the algorithm described by *King et al.* [1992] and *Platnick et al.* [2003]. These variables, as well as all other atmospheric properties from MODIS, are aggregated at daily, 8-day, and monthly time intervals on a global $1^\circ \times 1^\circ$ latitude-longitude grid. These level 3 products contain simple statistics (mean, standard deviation, etc.) computed for each parameter, and also contain marginal density and joint probability density functions between selected parameters [*King et al.*, 2003].

[12] MODIS aerosol and cloud properties have been validated by field experiments and intercomparisons with ground-based observations [*Chu et al.*, 2002; *Mace et al.*, 2005; *Kaufman et al.*, 2005]. Monthly mean aerosol and cloud products from Terra between April 2000 and September 2003 are utilized in the present study. In addition, daily cloud products from June to September 2001 are used for analysis of the weekly cycle of summertime urban aerosols.

2.2. EPA PM2.5 Data

[13] Because Terra/MODIS only provides daytime measurements of aerosol optical thickness at ~ 1030 local time (LT) for clear conditions, in situ EPA PM2.5 measurements are used to monitor the diurnal variation of aerosol concentration in this work. PM2.5 refers to particle mass of particles less than 2.5 μm diameter that generally consists of mixed solid and liquid aerosols in air and which excludes dust. PM2.5 therefore captures the mass of particles that are $\leq 2.5 \mu\text{m}$ in diameter.

2.3. AERONET Daily Data

[14] Aerosol Robotic Network (AERONET) provides ground-based aerosol monitoring and data archive at ~ 170 locations worldwide. Data of spectral aerosol optical thickness, size distribution, single scattering albedo, and precipitable water in diverse aerosol regions provide globally distributed near real time observations of aerosols [*Holben et al.*, 1998]. Hourly and daily AERONET measurements of aerosol optical thickness are used to identify the diurnal and weekly cycles of aerosol. The data are quality-ensured and cloud-screened [*Eck et al.*, 1999; *Smirnov et al.*, 2000].

2.4. TRMM Rainfall Data

[15] TRMM was launched in November 1997 as a joint U.S.-Japanese mission to advance the understanding of the global energy and water cycle by providing distributions of rainfall and latent heating over the global tropics [*Simpson et al.*, 1988; *Shepherd et al.*, 2002]. To extend TRMM data from 40°N – 40°S , we use the 3B-42 monthly, $1^\circ \times 1^\circ$ rain rate and rain accumulation product [*Adler et al.*, 2000]. This product uses TRMM microwave imager data to adjust merged infrared precipitation and root mean square precipitation error estimates. It should be noted that the quality of

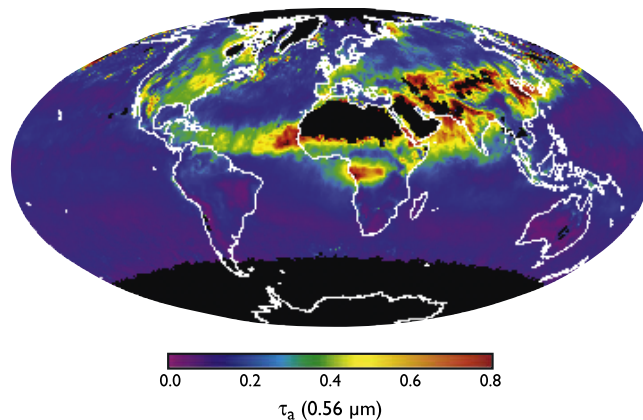


Figure 2. Monthly average aerosol optical thickness at 0.56 μm for January 2002. These data are produced at a $1^\circ \times 1^\circ$ latitude-longitude grid worldwide and are derived from Terra/MODIS measurements.

product 3B-42 is highly sensitive to the quality of the input infrared and microwave data. If the quality of the input data sources is less than anticipated, then the quality of product 3B-42 will be degraded. Nevertheless, these corresponding, multiyear rainfall products help establish the relationships between aerosols, clouds, and precipitation.

2.5. NDVI Data

[16] A 20-year NDVI data set derived from AVHRR channel 1 and channel 2 radiances is used to compare the vegetation/land cover changes in the New York and Houston regions. This data set is at 8 km and produced at a monthly resolution [*Tucker, 1979*].

2.6. NCEP Reanalysis

[17] The National Centers for Environmental Prediction (NCEP) Reanalysis and National Center for Atmospheric Research (NCAR) 50-year reanalysis [*Kistler et al.*, 2001] are used to reproduce the surface temperature and surface wind. The monthly averaged model output has a spatial resolution of $2.5^\circ \times 2.5^\circ$. The NCEP reanalysis, like any other GCM output, has uncertainties, but the overall geographical distribution is proven to be realistic, and therefore suitable for use in providing weather conditions for New York and Houston.

3. Results

3.1. Diurnal Variation

[18] Figure 2 shows the global distribution of aerosol optical thickness at 0.56 μm over both land and ocean for January 2002, except for locations where the surface is too bright to be able to retrieve the aerosol loading (e.g., Sahara, Saudi Arabia, Greenland). Urban regions of North America, Europe, India, and east Asia have larger aerosol optical thicknesses than most of the inner continents, with the exception of biomass burning in Gabon and the Democratic Republic of the Congo, and dust outbreaks from the Sahara that are transported across the Atlantic. As a consequence, the radiative forcing of aerosols is expected to be larger over urban areas than the inner continents where urban aerosols are largely absent. The maximum $\tau_a \sim 0.8$ occurs along the Ganges Valley of India, large portions of China, and the

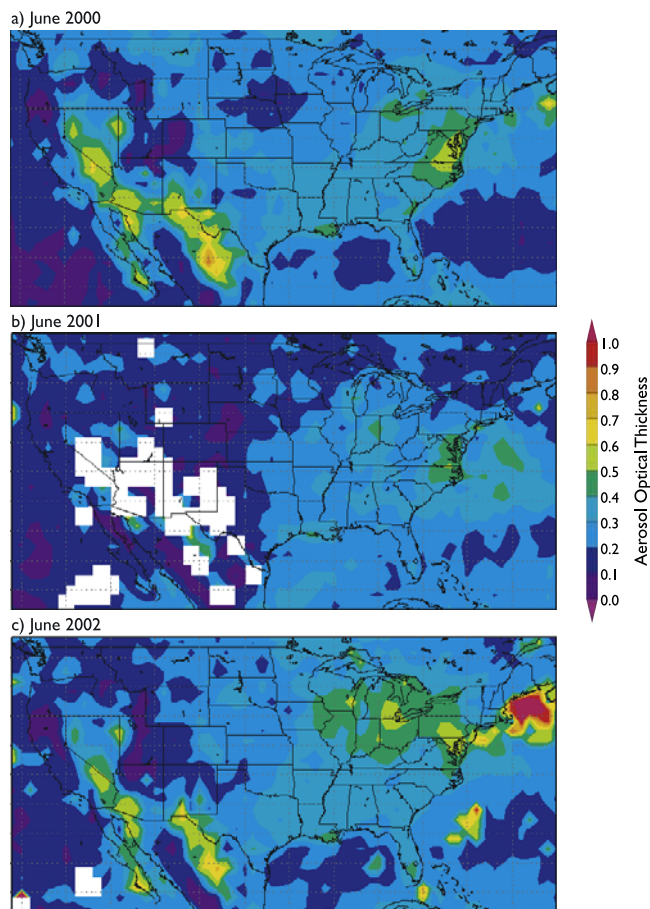


Figure 3. Spatial distribution of aerosol optical thickness for the United States. Observations are from Terra/MODIS for (a) June 2000, (b) June 2001, and (c) June 2002.

eastern United States. It should be emphasized that τ_a arises from all types of aerosols, not just those of anthropogenic origins from urban areas alone.

[19] Spatial values of τ_a ($0.56 \mu\text{m}$) change by 10% for the New York region in three consecutive summers. Values are above 0.5 in June 2000 and June 2002, but only around 0.4 in June 2001 (cf. Figure 3). Considering that the change is on a monthly mean scale, it is significant. In contrast, little change occurs in aerosol loading for three consecutive Junes in Houston, where $\tau_a \sim 0.3$ for all three Junes. Further study, as we will discuss below, suggests such differences are partly a result of local weather and climate conditions, and the subsequent transport of aerosols.

[20] Since a large portion of urban aerosols is attributed to anthropogenic activities, which have observed day and night differences, diurnal variation of aerosol loading is expected [Dickerson *et al.*, 1997; Smirnov *et al.*, 2002]. Aerosol concentration is also affected by boundary layer stability, which is stable at night and active during the daytime as a result of surface temperature increase [Stull, 1988]. Aerosol loading at the surface in urban areas is typically the smallest from late night to early morning (0300–0600 LT) and increases to the first maximum of the day at ~ 1000 LT and then drops slightly in the afternoon until the arrival of the second maximum of the day at about ~ 8 PM, as shown in Figure 4a. The peaks are likely

caused by early morning and late afternoon car combustion resulting from the rush hours. However, on most days, the diurnal cycle is strongly modified by weather conditions and is thus less typical than the classic case illustrated in Figure 4a, as implied by the error bars on the figures. Figure 4b shows that the peak aerosol quality index of Houston occurs around 1000 and 2100 EST, but attains a value of only 12, which is smaller than the 18 typical of New York. (Air quality index (AQI) is calculated by converting the measured pollutant concentrations into index values to report daily air quality. U.S. Environmental Protection Agency (EPA) calculates the AQI for five major air pollutants: ground-level ozone, particulate mass (PM), carbon monoxide, sulfur dioxide, and nitrogen dioxide. The AQI runs from 0 to 500. The higher the AQI value, the greater the level of air pollution and the larger the health concerns (see the EPA Web site for details www.epa.gov/airnow/aqi.html.) In addition, July monthly mean ozone in Houston has a similar diurnal pattern. Again, the large error bars suggest that the instantaneous aerosol and ozone loadings may significantly differ from the monthly average. Therefore a further look at daily variations will help illustrate the ranges and reasons for the diurnal behavior of urban aerosols.

[21] One-day measurements from AERONET for the Goddard Institute for Space Studies (GISS), located in New York City (Figure 5b), show that on 15 July 2001 there was a sharp increase in spectral aerosol optical

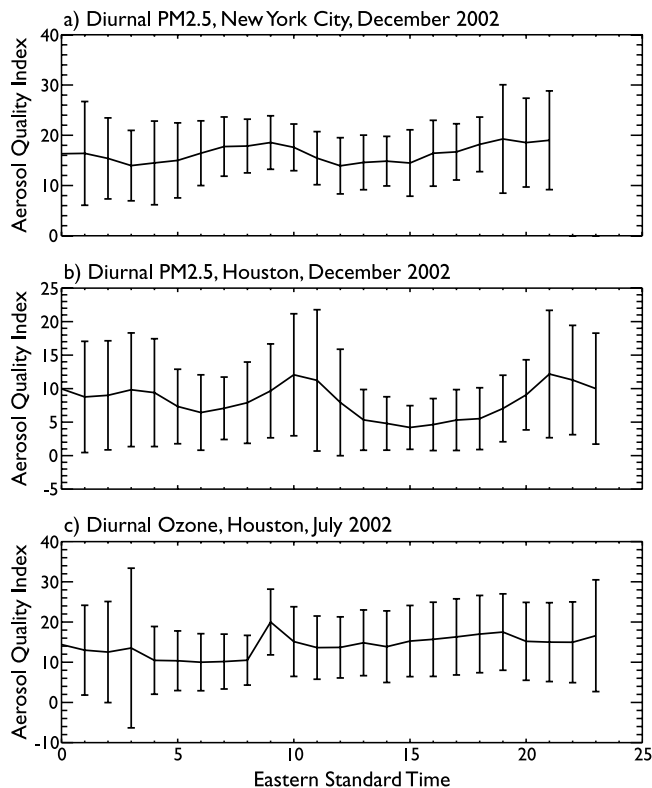


Figure 4. Monthly mean diurnal variations of urban aerosol for New York and Houston. Data are obtained from EPA (a) monthly mean aerosol quality index for PM_{2.5} in New York City, December 2002; (b) PM_{2.5} for December 2002 in Houston; and (c) Ozone for July 2002 in Houston. Error bars shown are standard deviations. See text for details.

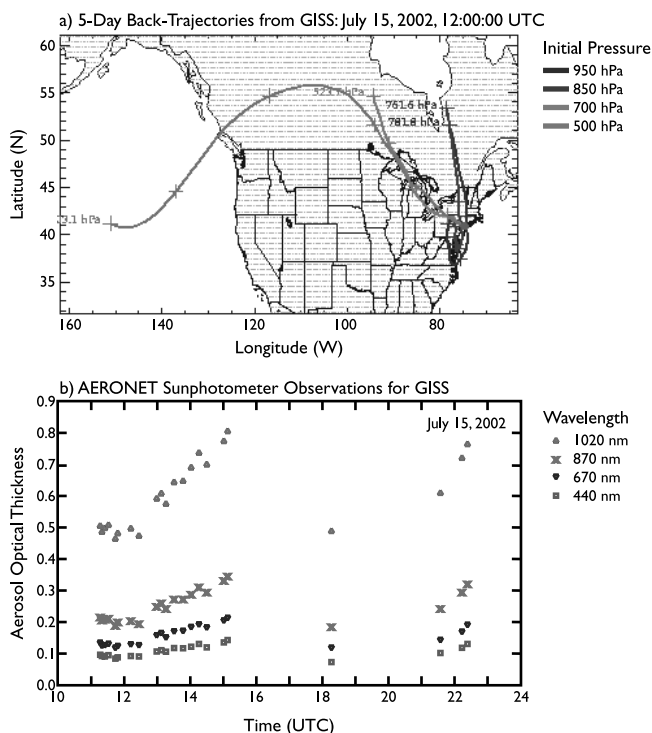


Figure 5. Diurnal variation of aerosol optical thickness for New York City on 15 July 2002. Data are based on AERONET GISS station measurements: (a) back-trajectory analysis provided by Anne Thompson (NASA/GSFC) and (b) AERONET-measured aerosol optical thickness. (Sources: images are produced and available at www.aeronet.gsfc.gov.)

thickness, from 0.5 at noon to 0.8 at 3 PM UTC, for 1020 nm wavelength. The corresponding 7-day back-trajectory analysis of AERONET (Figure 5a) reveals that the original aerosols were transported from northern Canada. These transported aerosols are likely products of the Canadian forest fires that started over central Quebec during the period 5–9 July 2002 [Colarco *et al.*, 2004], because at the 850 and 950 hPa pressure levels, the parcels transported to New York City were originally around the Quebec fire locations five days earlier (Figure 5a). The back trajectories were derived from the NASA GSFC trajectory model [Schoeberl and Sparling, 1995; Thompson *et al.*, 2002], which uses the wind information provided by NCEP and NCAR reanalysis [Kistler *et al.*, 2001].

[22] However, day-to-day aerosol variation is significant: on calm, clear days such as 2, 6, and 7 July 2001 (not shown), the diurnal aerosol optical thickness is smooth and as low as 0.04. By contrast, aerosol optical thickness on 3 and 5 July 2001 was 0.06–0.08 in late morning and slightly increased in the late afternoon before the occurrence of clouds inhibited further measurements (not shown). Unlike variations at other longer timescales, the diurnal variation of aerosols is strongly controlled by local weather conditions, such as wind, which enhances the aerosol transport.

3.2. Seasonal and Interannual Variations

[23] Pronounced seasonality with a minimum in winter and a maximum in April to early summer is observed in

both New York City and Houston based on Terra/MODIS level 3 data analysis for 3 years (cf. Figure 6). For Houston, the minimum monthly mean aerosol optical thickness is <0.2 in the four continuous years from 2000 to 2003, although the occurrence time of the minimum differs slightly: December in 2000, December to January in 2001, and November to January in 2002. The maxima are above 0.4 with the extreme value as high as 0.52 in April 2000. The occurrence of the maxima in April or May is hypothesized to correspond to the peak time of annual biomass burning in Mexico [Duncan *et al.*, 2003]. For New York, large-scale frontal or jet stream weather systems are typically active during this transitional season, transporting the biomass burning–emitted aerosols from Canada to New York City and through turbulent planetary boundary layer (PBL) mixing of upper altitude-transported aerosols to the surface. By contrast, the minimum τ_a (0.56 μm) in New York is 0.15, lower than that of Houston, and the maximum τ_a is above 0.5, consistent with that of Houston. Note that New York’s January 2001 has a peak aerosol optical thickness while other Januarys have low optical thickness. Further examination of the daily observations of AERONET and the NCEP reanalysis suggest that this peak in January 2001 may be an error in data analysis.

3.3. Weekly Variation

[24] Previous research on urban pollutant transport revealed a weekday-weekend differences in ozone, nitrogen oxide, and nonmethane hydrocarbons in California [Marr and Harley, 2002a, 2002b], as a result of vehicle emissions.

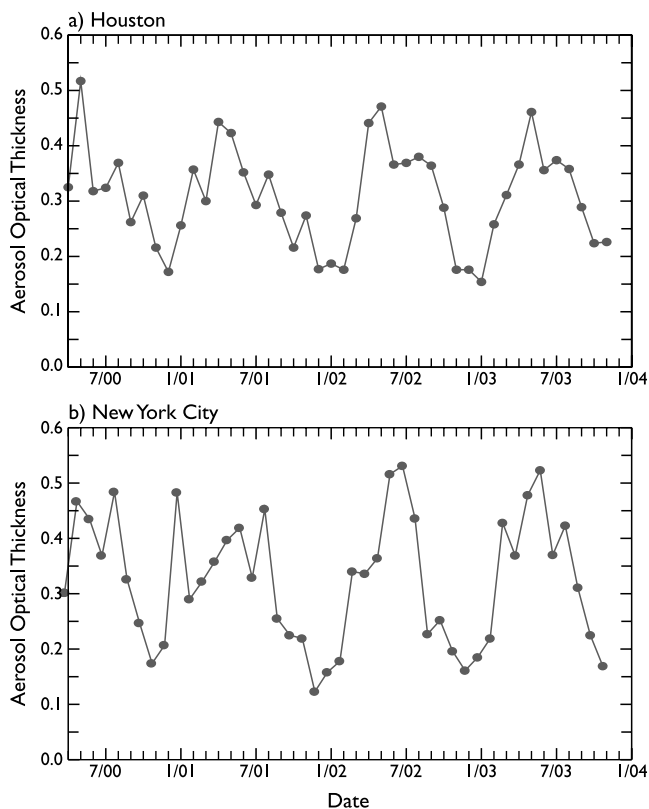


Figure 6. MODIS-derived monthly mean aerosol optical thickness at 0.56 μm from April 2000 to September 2003 for (a) Houston and (b) New York City.

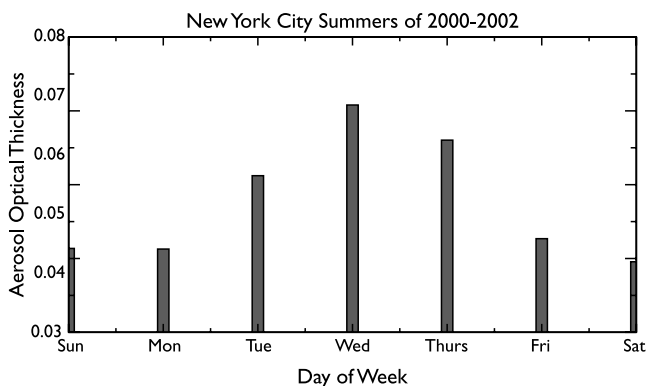


Figure 7. Averaged weekly distribution of aerosol optical thickness based on AERONET data from the GISS station (41°N , 74°W). Data are from August–September 2000, June–September 2001, and June–September 2002. To minimize transport effects, for each day, only observations within late afternoon hours after 1700 are used to calculate the daily average. Only daily averages smaller than 0.15 are used to analyze the weekly variation.

Specifically, emissions of NO_x on weekends are about 30% less than on weekdays due to a large decrease of heavy-duty truck activity. This has also been observed from satellite observation [cf. *Beirle et al.*, 2003]. As a result, higher O_3 was observed during the weekend than on weekdays due to a series of chemical processes that produce O_3 from NO_x [*Dickerson et al.*, 1997]. Such weekly variation has been called the “weekend effect” [*Marr and Harley*, 2002b], which was originally reported in the 1970s [*Lebron*, 1975] and has been detected in New York City, Los Angeles, St. Louis, Vancouver, San Francisco, and Switzerland [*Cleveland et al.*, 1974; *Lonneman et al.*, 1974; *Elkus and Wilson*, 1977].

[25] Research on rainfall over New York and surrounding oceanic regions also shows larger weekend rainfall than weekdays (so-called “wet Saturday,” *Cerveny and Balling* [1998]). Aerosols’ weekly variations were attributed to such rainfall weekly differences [*Cerveny and Balling*, 1998]. Similarly, based on multiyear TRMM rainfall measurements, weekly cycles have been identified for many regions of the Northern Hemisphere for summer time, although the weekly signal is so weak that it may not be detectable for one specific year (T. L. Bell, personal communication, 2004).

[26] To address if a weekly cycle in urban aerosols indeed exists and how strong this signal is, we examined the three continuous summers (2000, 2001, 2002) using daily AERONET in situ measurements. Correspondingly, we use MODIS cloud properties to examine if the weekly cycle is resolvable in the clouds fields.

[27] The weekly cycle of aerosol optical thickness over New York City as derived from AERONET observations (Figure 7) shows high values during weekdays and low values on weekends. The peak appears on Wednesday. This is consistent with previous urban aerosol reports [*Marr and Harley*, 2002a, 2002b; *Linacre and Geerts*, 2002]. Daily data for August–September 2000, June–September 2001, and June–September 2002 from the AERONET GISS station have been sampled. Several average and filtering

methods were tested to examine whether the weekly cycle signal is present. We notice that τ_a over New York City can range from 0.02 to 0.8, depending on surface traffic and overlying atmospheric winds. To reduce the high τ_a transported from outside of the city, we only selected the days having $\tau_a < 0.17$. In addition, we only sampled the measurements taken during the late afternoon and afterward because urban surfaces have warm anomalies as compared to the surrounding regions (i.e., urban heat island effect) and thus result in active convection in the early afternoon. Consequently, the urban atmospheric column would be less stable than the surrounding areas, indicating a higher probability of the city-induced convective activities that disturb surface aerosol concentration [*Shepherd et al.*, 2002, *Shepherd and Burian*, 2003].

[28] The signals of weekly variation are distinct from year to year, as shown in Figure 8 in terms of median of all the samples. Summer 2001 has a stronger signal with the overall $\tau_a \geq 0.04$ and the average Wednesday value is above 0.07. By comparison, in 2000 and 2002 summer, the weekday-weekend differences are smaller. This suggests that the weekly cycle is very weak and may not be valid for all years, but further study is warranted.

[29] Correspondingly, a weekly cycle of cloud properties is also evident (Figure 9), with water cloud effective radius peaking on Wednesday and liquid water path peaking on weekends. These data were derived from daily Terra/MODIS level 2 cloud observations using the algorithm described by *Platnick et al.* [2003]. Again, these weekly cycles may be a result of human activities since no natural forcing has a 7-day cycle in summer midlatitudes.

[30] Weekday-high aerosol optical thickness and weekend-high cloud liquid water path are detectable for Houston as well, but these signals are relatively weak (not shown). This is partly because the surface transport over Houston is generally stronger than in New York, which distributes urban aerosols to other regions rapidly. In addition, the larger surface temperature in a subtropical city may induce stronger surface layer and boundary layer mixing, which

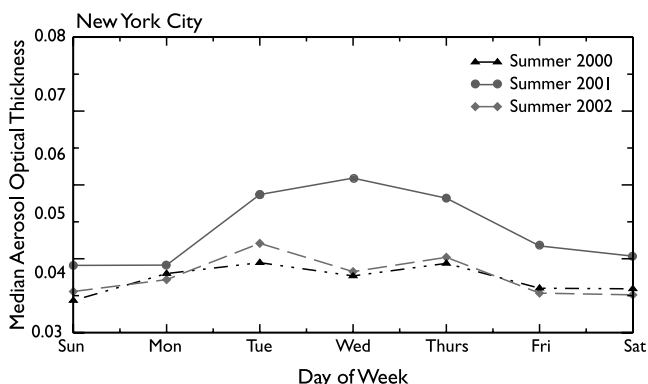


Figure 8. Weekly variations of aerosol optical thickness for summers of years 2000, 2001, and 2002. Owing to data availability, summer 2000 includes samples for August–September, summer 2001 for June–September, and summer 2002 for June–September 2002. Data were obtained from the AERONET GISS station in New York City (41°N , 74°W). To reduce aerosol influence transported from high out-of-city sources, only $\tau_a < 0.17$ was analyzed here.

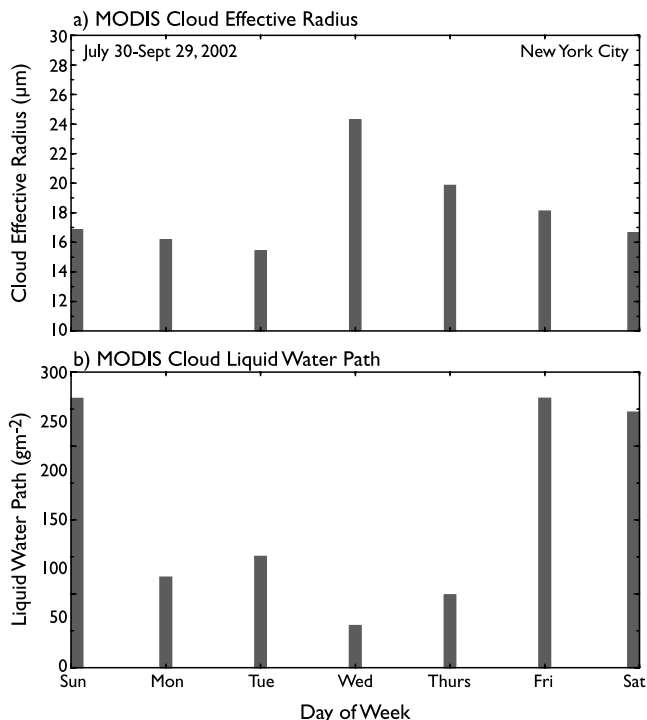


Figure 9. Weekly distribution of (a) cloud effective radius and (b) cloud-integrated water path for New York City (41°N , 74°W). The data represent the median of the daily averages of June to September 2001 that are then spatially averaged over a $50\text{ km} \times 50\text{ km}$ region centered on New York City, based on the MODIS 1-km resolution level 2 data.

transports surface aerosols to the free atmosphere faster than at midlatitude cities [Jin *et al.*, 2005].

3.4. Aerosol-Cloud-Rainfall Relationships

[31] For Houston, the interannual cloud optical thickness has its minima during summers and maxima during winters, and ranges from 5 to 25 (Figure 10b). In addition, for water clouds, effective cloud droplet size has an opposite phase to cloud optical thickness. Namely, thick aerosols correspond to high droplet size and low cloud optical thickness. At first sight, these results seem to be inconsistent with the Twomey effect: when there are more aerosols, aerosols serve as CCN and reduce the size of cloud effective radius (cf. Figure 10b), and thus increases cloud optical thickness when the liquid water path of the atmosphere layer does not change [Twomey, 1977]. However, the Twomey theory assumes that the liquid water content in clouds does not change. Therefore Figure 10 is not suitable to examine the Twomey theory (S. Platnick, personal communication, 2004). Several processes might be responsible for the consistent phase of aerosols and water cloud effective radius observed in Figure 10: in Houston a significant portion of aerosols are likely transported from the sea, and sea salt aerosols have large size and may serve as nuclei to form some of the cloud droplets that are much larger than the average size [Rogers and Yau, 1989]. Another reason is that more aerosols correspond to smaller ice cloud particle size (not shown), which suggests that urban aerosols may serve as CCN and reduce cloud base droplets' size due to evap-

oration [Twomey, 1977], and these smaller water droplets are relatively easily lifted to higher altitudes to become ice clouds and thus reduce the averaged ice cloud effective radius [Rosenfeld, 2000]. A third explanation is that chemical processes may also be responsible for the opposite phase of aerosol and cloud effective radius [Rissman *et al.*, 2004].

[32] Urban-induced changes to clouds can be detected from the difference of cloud properties over urban and nearby nonurban regions. Figure 11 shows that in summer, water clouds over the Houston region have smaller effective radii than clouds located east and south of Houston, and have larger effective radius than clouds located west and north of Houston. We focus on summer when mesoscale forcing is more dominant than large-scale, strongly forced events (e.g., frontal systems) over urban regions. Urban aerosols are part of the reason for the differences in cloud effective radius. Although the eastern, western, northern, and southern regions of Houston are only displaced 1° ($\sim 100\text{ km}$) from the Houston region, the thermodynamic and kinetic conditions in the environment are quite different as seen from the monthly mean July surface pressure field (not shown). The surface wind is from south to north with high pressure centered to the east. This configuration transports urban aerosols to the northern and western regions, which may explain why these regions have smaller cloud effective radius than the regions to the east and south of Houston. Furthermore, Houston and surrounding regions all have consistent seasonality on cloud effective radius.

[33] Seasonality of cloud top temperature for water clouds is similar to that of aerosol optical thickness, namely, low values in winter months and high values in summer months (Figure 12), for both New York City and Houston. This implies that a low aerosol optical thickness corresponds to cold water clouds and a high optical thickness corresponds to warm water clouds. A hypothesis is that strong boundary layer mixing transports surface aerosols to high altitude which can further be removed from the city through high level winds; this reduces aerosol optical thickness; meanwhile, stronger vertical mixing moves cloud

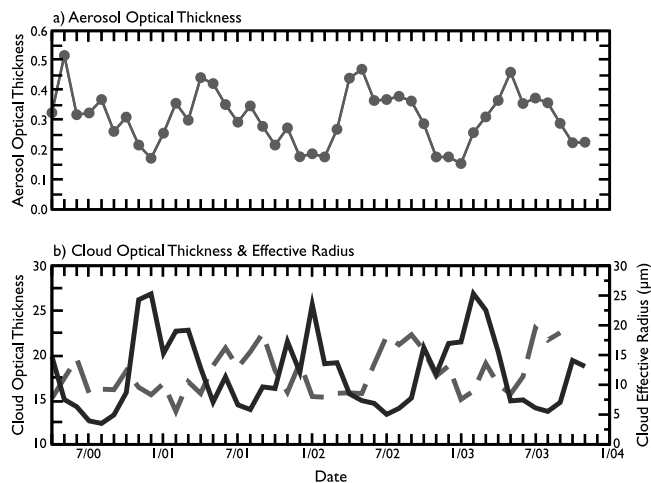


Figure 10. MODIS-derived relationship between (a) aerosol optical thickness at $0.56\text{ }\mu\text{m}$ and (b) water cloud optical thickness (solid) and effective radius (dashed) for Houston.

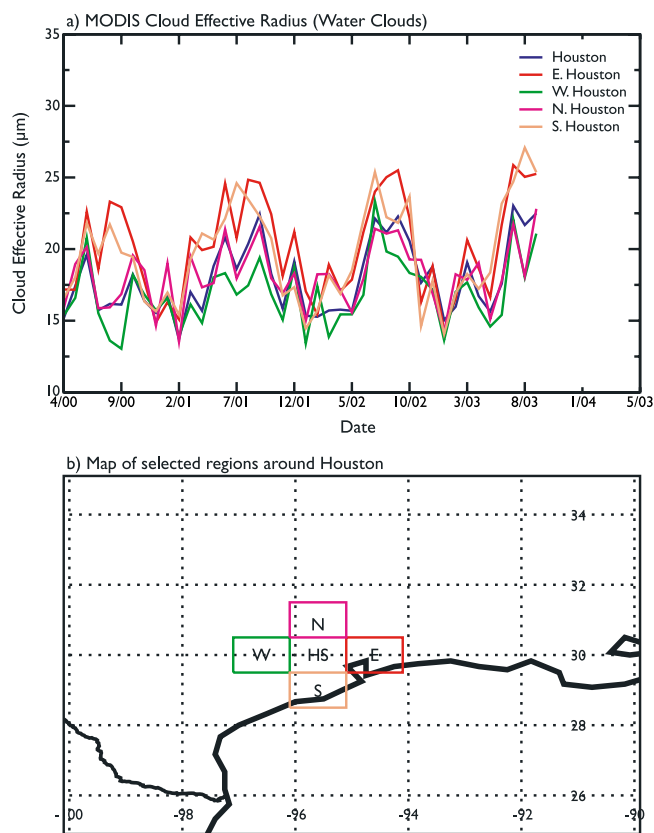


Figure 11. (a) MODIS-derived monthly mean water cloud effective radius for Houston, and east, south, west, and north of Houston. (b) The map for the selected regions of Houston, and east, south, north, and south of Houston. Houston is located from 29° – 30° N and 74° – 75° W. All five regions are $1^{\circ} \times 1^{\circ}$ boxes.

droplets to colder altitudes causing lower cloud top temperature. On the contrary, modest vertical mixing helps keep aerosols at the surface layer for a high aerosol optical thickness and low cloud top temperature. In addition, sea salt aerosols may play a role, but currently there are no reliable measurements for examining sea salt aerosols as even the MODIS aerosol coarse fraction has large uncertainty and thus is unsuitable for detecting the slight signal of sea salt aerosols over land (Y. J. Kaufman, personal communication, 2004).

[34] Little seasonality is observed for rainfall over Houston and New York City, suggesting that rainfall is less directly affected by aerosols than are clouds (Figure 13). Around Houston, the TRMM-based accumulated rainfall data show that the maxima monthly mean rainfall occurs in October 2000, May 2001, and September 2002, above 200 mm per month. This is consistent with the transition τ_a seasons in this region. In general, New York's rainfall has less month-to-month variation than Houston's, with a maximum slightly above 200 mm/month in October 2002. Consequently, effective radius for water clouds is lower in New York City than in Houston (Figure 14a), implying a larger aerosol amount in New York City than in Houston, which is consistent with results previously reported in Figures 3 and 6. It seems that with the increase of cloud

effective radius for water clouds, accumulated rainfall increases (Figure 14a). There are no inherent relations between aerosols and precipitation amount. More precipitation occurs typically with deeper clouds. The effective radius increases with cloud depth. This may be the primary cause of the positive relation in Figure 14a. In contrast, Figure 14b is for ice clouds, which again show little relationship between effective radius and accumulated rainfall.

[35] Analyzing monthly mean aerosol optical thickness versus rainfall identifies little one-to-one relationship in a climatological sense. In Figure 15a, the correlation coefficients between τ_a and monthly mean accumulated rainfall over the whole year are 0.18 for New York and -0.17 for Houston, while over summer months (Figure 15b) they are 0.27 for New York and 0.02 for Houston, respectively. Such low correlation indicates no statistically meaningful relationship exist in monthly mean aerosol τ_a and rainfall amount, suggesting the aerosol is not the primary reason for the urban-induced rainfall modification observed by *Shepherd et al.* [2002]. *Shepherd and Burian* [2003] reported urban-induced rainfall anomalies over and downwind of Houston. Understanding the mechanism responsible for rainfall anomalies is essential to simulating them in GCMs. The less direct relationship between rainfall and aerosol optical thickness as presented in Figure 15 implies that urban rainfall anomalies are not fully related to aerosol change. This observation is consistent with the recent hypothesis of *Shepherd and Burian* [2003] that dynamic

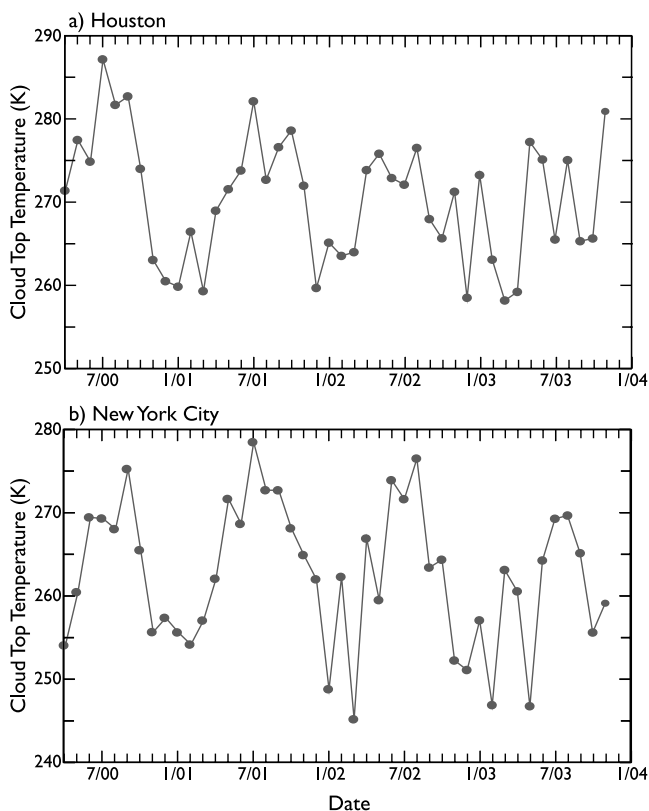


Figure 12. Comparison of cloud top temperature of (a) Houston and (b) New York City derived from Terra/MODIS data.

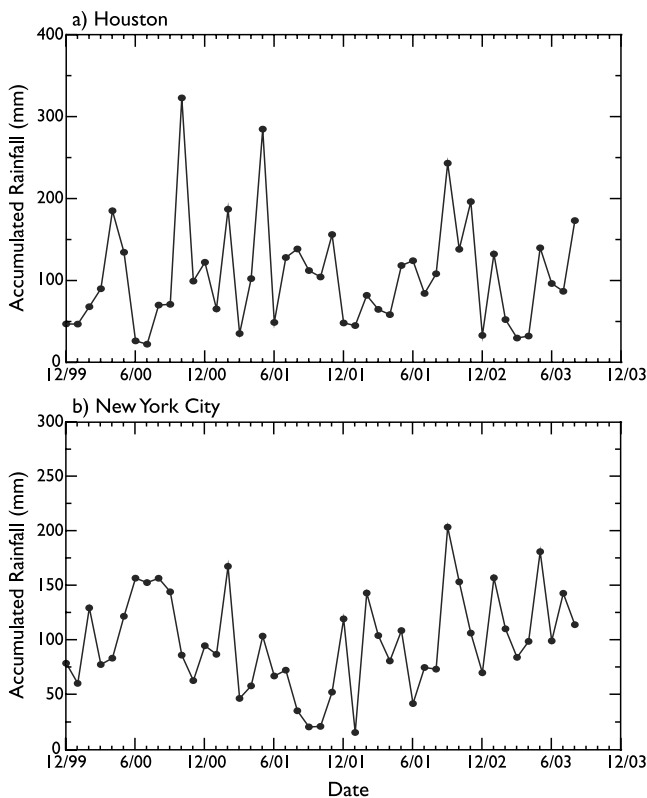


Figure 13. TRMM observed monthly mean rainfall for (a) Houston and (b) New York City from January 2000 to September 2003. The observation product is 3B42 at 1° resolution.

processes like surface convergence and boundary destabilization are more dominant than aerosols for urban-induced convective events.

4. Background Conditions of New York and Houston

[36] The urban aerosols and their effects vary from one city to another, depending on the city's microstructure (e.g., land use, building density, population density, and living styles), seasons, and prevailing environmental forcing [Oke, 1982; Karl *et al.*, 1988; Jin *et al.*, 2005]. To understand aerosol and cloud differences between New York and Houston, some knowledge of the human population, land cover and land use, and large or regional-scale weather systems for these two regions is essential.

[37] Table 1 is the human population, population density, and population change from 1990 to 2000. New York City has a larger population than Houston, and consequently has more intense human activities and anthropogenic aerosol concentration as shown in Figures 3, 6, and 14a. Specifically, New York has a population of 8,008,278 with a population density of 26,401 people per square mile, while Houston has only 1,953,631 people with a population density of 3,372 people per square mile (2000 census). This difference might contribute to the factors causing New York to have higher τ_a than Houston in the summer months (Figure 6). Houston population grew faster than New York City from 1990 to 2000: New York increased by 9% and Houston increased by 19%.

[38] Figure 16 shows the difference in the NDVI between July 1981 and July 2000. Both New York City and Houston have experienced significant land cover changes from 1980 to 2000, with corresponding changes in surface greenness, as indicated in NDVI. New York City and its surrounding region seem to have experienced a slightly larger NDVI change over the past 20 years as compared to Houston.

[39] Figure 17 presents the monthly surface wind field based on NCEP reanalysis. In general, surface wind is affected by topography and thus may not exactly follow the pressure system. In July, the Houston area is influenced by high pressure over the sea that advects wind from the ocean to land. During this time period, Houston's surface circulation is dominated by more mesoscale circulations such as sea, bay, and heat island circulations, whereas New York's surface wind comes from the southwest (mostly land cover). This implies that Houston may have larger sea salt aerosols than New York, as ocean sea salt aerosols are transported into the city.

5. Final Remarks

[40] Clearly, the dramatic increase and expansion of human activities in the past century has led to significant changes in land use and possible influences on the regional to global climate. Specifically, construction of new buildings and roads tends to disturb the natural land and vegetation morphology and enhance the surface frictional

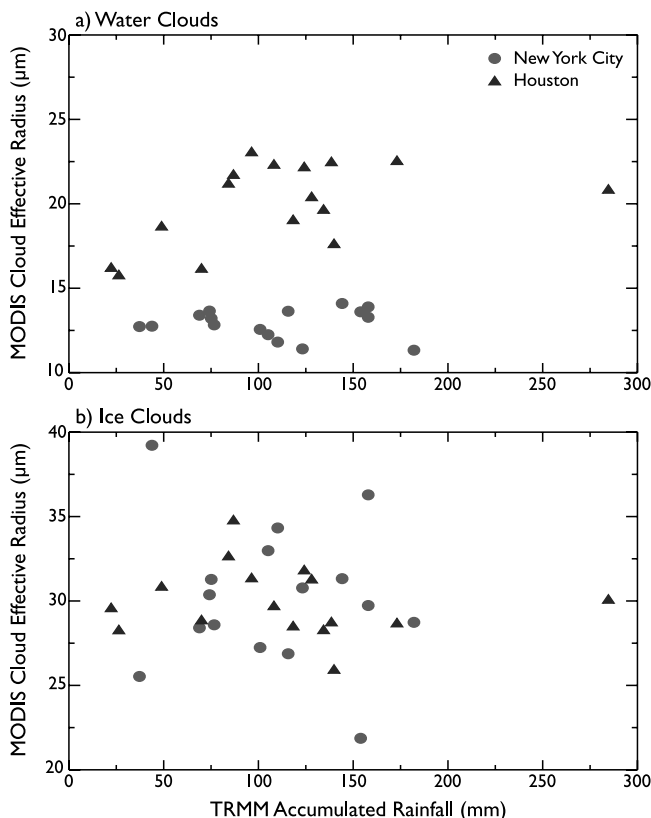


Figure 14. Monthly mean accumulated rainfall versus cloud effective radius for New York City and Houston (a) for water clouds and (b) for ice clouds. Only summer months (June–September) for 2000–2003 are analyzed.

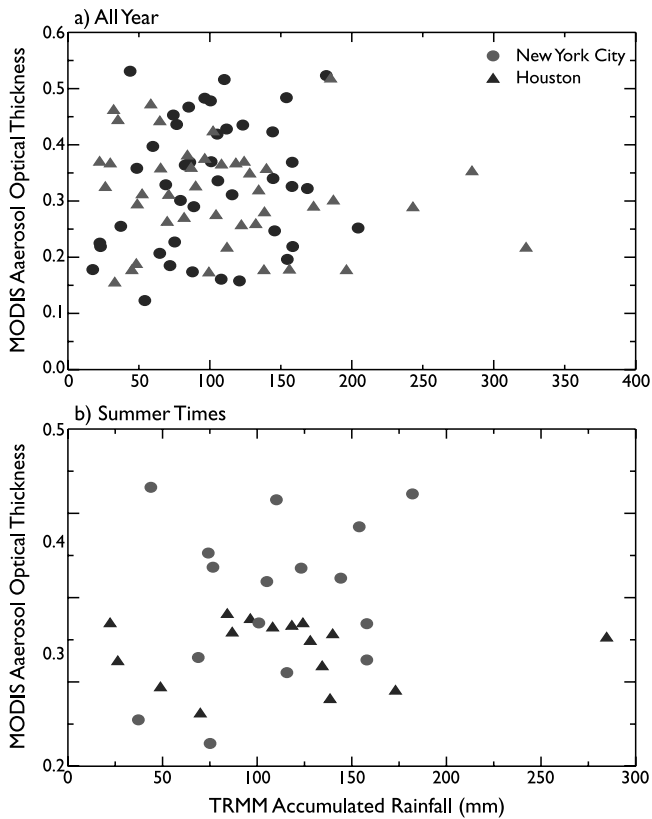


Figure 15. The scatterplot of MODIS aerosol thickness and TRMM-based accumulated rainfall for Houston and New York City, respectively: (a) all months within April 2000 to December 2003 and (b) is summer months, namely, the warm season period (June–September) for 2000, 2001, 2002, and 2003.

effects on the atmospheric flows above. The resulting dynamical effects are to weaken surface flows but to increase the upward turbulent transport of aerosols.

[41] This research reveals that spatial and temporal urban aerosols vary dynamically as a result of various parallel factors, such as human activity, land cover changes, cloud-aerosol interactions, and chemical processes. Aerosol variations affect surface insolation, which in turn affect surface temperature. In a normal day of September, the aerosol-induced decrease of surface insolation is $20\text{--}30\text{ Wm}^{-2}$ (cf. Figure 2). Therefore, for dense urban regions, surface temperature studies need to take into account the aerosol factor.

[42] Diurnal, seasonal, and interannual variations of aerosols have been examined using satellite, surface, and NCEP reanalysis data. Diurnal variations of aerosols are largely affected by weather conditions, but τ_a often peaks during

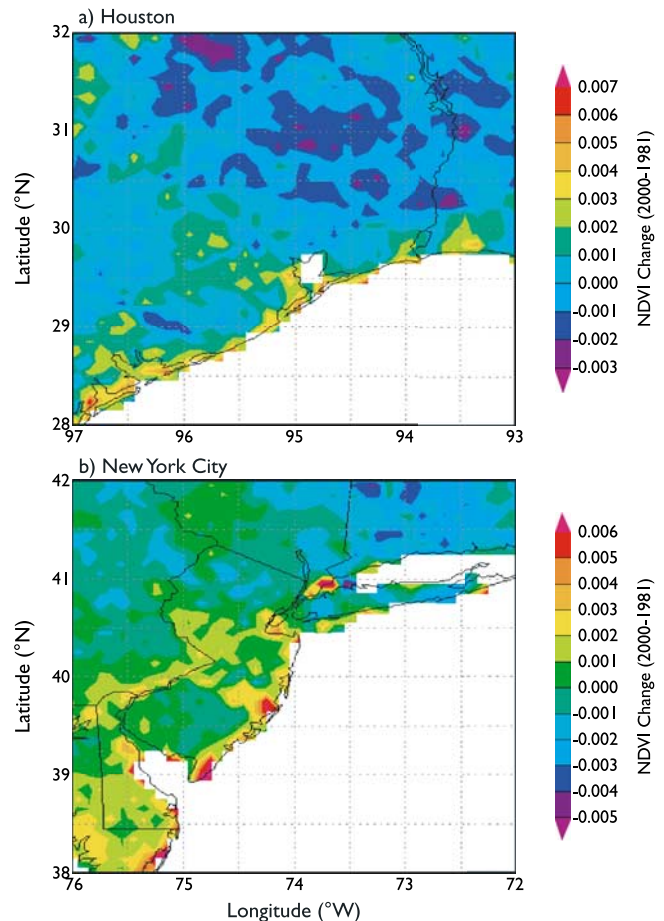


Figure 16. NDVI changes from 1981 to 2000 for (a) Houston and (b) New York City. Anomalies are calculated using NDVI for 2000 minus the NDVI climatology, which is the averaged NDVI from 1980 to 2000.

the rush hours in the morning and evening. In addition, seasonality of aerosol optical thickness has an opposite phase when compared to cloud optical thickness and little relationship with rainfall. Weekly cycles of urban aerosols and clouds, in particular, have been observed for the first time in New York. This cycle may be interpreted as a signal of human activities. Nevertheless, this cycle may not be significant in other cities where aerosol transport is strong (like Houston), which implies this cycle is weaker than other temporal properties. By all means, the weekly cycle shows a possible human footprint on the local atmosphere-surface system, and is only statistically valid.

[43] The above results have important implications with respect to the modeling of aerosols, clouds, and rainfall. Specifically, high-resolution satellite observations of aero-

Table 1. Population and Population Density for New York City and Houston^a

City Name	2000 Population	2000 Land Area, mile ²	2000 Population Density, mile ⁻²	1990 Population	1990 Land Area, mile ²	1990 Population Density, mile ⁻²	Change in Population, %
New York City	8,008,278	303.3	26,401	7,322,564	308.9	23,705	9
Houston	1,953,631	579.5	3,372	1,630,553	539.9	3,020	19

^aSource: U.S. 2000 census from www.demographia.com/db-2000city50kdens.htm.

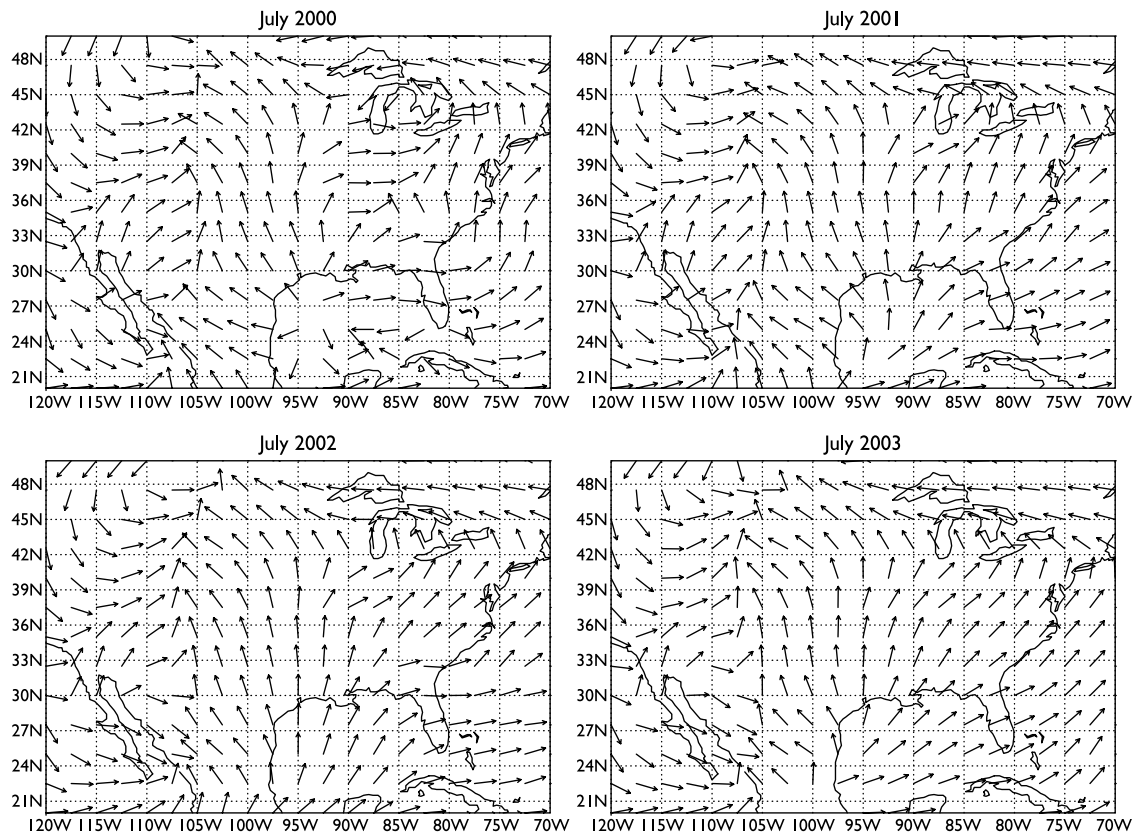


Figure 17. Monthly mean surface wind for July 2000, July 2001, July 2002, and July 2003. The data are from NCEP/NCAR reanalysis at $2.5^\circ \times 2.5^\circ$.

sols, clouds, and rainfall could be used to update the atmospheric parameters for both numerical weather prediction and global (regional) climate models [Jin and Shepherd, 2005]. The global distributions of aerosols and clouds could be utilized to initialize these models or validate the realisms of different model cloud microphysical processes.

[44] **Acknowledgments.** We thank Brent Holben and the AERONET staff for the user-friendly online data archive and analysis system in support of AERONET. We also thank Zhong Liu for developing an efficient online tool for MODIS, NDVI, and TRMM data. Special thanks go to Ming-Dah Chou for helpful discussions on his radiative transfer model. We appreciate the NOAA-CIRES Climate Diagnostics Center for online data retrieval and image. This work was funded by the NASA TRMM project under contract PMM-0022-0069.

References

- Adler, R. F., G. J. Huffman, D. T. Bolvin, S. Curtis, and E. J. Nelkin (2000), Tropical rainfall distributions determined using TRMM combined with other satellite and rain gage information, *J. Appl. Meteorol.*, *39*(12), 2007–2023.
- Arnfield, A. J. (2003), Two decades of urban climate research: A review of turbulence, exchanges of energy and water, and the urban heat island, *Int. J. Clim.*, *23*, 1–26.
- Beirle, S., U. Platt, M. W6nig, and T. Wagner (2003), Weekly cycle of NO_2 by GOME measurements: A signature of anthropogenic sources, *Atmos. Chem. Phys.*, *3*, 2225–2232.
- Cervený, R. S., and R. C. Balling Jr. (1998), Weekly cycles of air pollution, precipitation and tropical cyclones in the coastal NW Atlantic region, *Nature*, *394*, 561–563.
- Changnon, S. A. (1978), Urban effects on severe local storms at St. Louis, *J. Appl. Meteorol.*, *17*, 578–592.
- Changnon, S. A. (1992), Inadvertent weather modification in urban areas: Lessons for global climate change, *Bull. Am. Meteorol. Soc.*, *73*, 619–627.
- Chou, M. D., and M. J. Suarez (1999), A solar radiation parameterization for atmospheric studies, *NASA Tech. Memo 104606*, vol. 15, 40 pp., Greenbelt, Md.
- Chu, D. A., Y. J. Kaufman, C. Ichoku, L. A. Remer, D. Tanré, and B. N. Holben (2002), Validation of MODIS aerosol optical depth retrieval over land, *Geophys. Res. Lett.*, *29*(12), 8007, doi:10.1029/2001GL013205.
- Chu, D. A., Y. J. Kaufman, G. Zibordi, J. D. Chern, J. Mao, C. Li, and B. N. Holben (2003), Global monitoring of air pollution over land from the Earth Observing System-Terra Moderate Resolution Imaging Spectroradiometer (MODIS), *J. Geophys. Res.*, *108*(D21), 4661, doi:10.1029/2002JD003179.
- Cleveland, W. S., T. E. Graedel, B. Kleiner, and J. L. Warner (1974), Sunday and weekday variations in photochemical air pollutants in New Jersey and New York, *Science*, *186*, 1037–1038.
- Colarco, P. R., M. R. Schoeberl, B. G. Doddridge, L. T. Marufu, O. Torres, and E. J. Welton (2004), Transport of smoke from Canadian forest fires to the surface near Washington, D.C.: Injection height, entrainment, and optical properties, *J. Geophys. Res.*, *109*, D06203, doi:10.1029/2003JD004248.
- Dickerson, R. R., S. Kondragunta, G. Stenchikov, K. L. Civerolo, B. G. Doddridge, and B. N. Holben (1997), The impact of aerosols on solar ultraviolet radiation and photochemical smog, *Science*, *278*, 827–830.
- Duncan, B. N., R. V. Martin, A. C. Staudt, R. Yevich, and J. A. Logan (2003), Interannual and seasonal variability of biomass burning emissions constrained by satellite observations, *J. Geophys. Res.*, *108*(D2), 4100, doi:10.1029/2002JD002378.
- Eck, T. F., B. N. Holben, J. S. Reid, O. Dubovik, A. Smirnov, N. T. O'Neill, I. Slutsker, and S. Kinne (1999), Wavelength dependence of the optical depth of biomass burning, urban, and desert dust aerosols, *J. Geophys. Res.*, *104*(24), 31,333–31,349.
- Elkus, B., and K. R. Wilson (1977), Photochemical air pollution: Weekend-weekday differences, *Atmos. Environ.*, *11*, 509–515.
- Ghan, S., R. Easter, J. Hudson, and F. Br6on (2001), Evaluation of aerosol indirect radiative forcing in MIRAGE, *J. Geophys. Res.*, *106*(D6), 5317–5334.
- Grimmond, C. S. B., and T. R. Oke (1995), Comparison of heat fluxes from summertime observations in the suburbs of four North American cities, *J. Appl. Meteorol.*, *34*, 873–889.

- Hansen, J., M. Sato, and R. Ruedy (1997), Radiative forcing and climate response, *J. Geophys. Res.*, *102*, 6831–6864.
- Holben, B. N., et al. (1998), AERONET—A federated instrument network and data archive for aerosol characterization, *Remote Sens. Environ.*, *66*, 1–16.
- Huff, F. A., and J. L. Vogel (1978), Urban, topographic and diurnal effects on rainfall in the St. Louis region, *J. Appl. Meteorol.*, *17*, 565–577.
- Intergovernmental Panel on Climate Change (IPCC) (2001), *Climate Change 2001: The Scientific Basis, Contribution of Working Group I to the Third Assessment Report of the Intergovernmental Panel on Climate Change*, edited by J. T. Houghton et al., 881 pp., Cambridge Univ. Press, New York.
- Jin, M. (2000), Interpolation of surface radiation temperature measured from polar orbiting satellites to a diurnal cycle. Part 2: Cloudy-pixel treatment, *J. Geophys. Res.*, *105*(D3), 4061–4076.
- Jin, M. (2004), Analysis of land skin temperature using AVHRR observations, *Bull. Am. Meteorol. Soc.*, *85*, 587–600.
- Jin, M., and R. E. Dickinson (1999), Interpolation of surface radiation temperature measured from polar orbiting satellites to a diurnal cycle. Part 1: Without clouds, *J. Geophys. Res.*, *104*, 2105–2116.
- Jin, M., and R. E. Dickinson (2000), A generalized algorithm for retrieving cloudy sky skin temperature from satellite thermal infrared radiances, *J. Geophys. Res.*, *105*, 27,037–27,047.
- Jin, M., and R. E. Dickinson (2002), New observational evidence for global warming from satellite, *Geophys. Res. Lett.*, *29*(10), 1400, doi:10.1029/2001GL013833.
- Jin, M., and J. M. Shepherd (2005), On including urban landscape in land surface model—How can satellite data help?, *Bull. Am. Meteorol. Soc.*, in press.
- Jin, M., R. E. Dickinson, and D. Zhang (2005), The footprint of urban climate change through MODIS, *J. Clim.*, in press.
- Karl, T. R., H. F. Diaz, and G. Kukla (1988), Urbanization: Its detection and effect in the United States climate record, *J. Clim.*, *1*, 1099–1123.
- Kaufman, Y. J., D. Tanré, L. A. Remer, E. F. Vermote, A. Chu, and B. N. Holben (1997), Operational remote sensing of tropospheric aerosol over land from EOS Moderate Resolution Imaging Spectroradiometer, *J. Geophys. Res.*, *102*, 17,051–17,067.
- Kaufman, Y. J., D. Tanré, and O. Boucher (2002), A satellite view of aerosols in the climate system, *Nature*, *419*, 215–223.
- Kaufman, Y. J., I. Koren, L. A. Remer, D. Tanré, P. Ginoux, and S. Fan (2005), Dust transport and deposition observed from the Terra-Moderate Resolution Imaging Spectroradiometer (MODIS) spacecraft over the Atlantic Ocean, *J. Geophys. Res.*, *110*, D10S12, doi:10.1029/2003JD004436.
- King, M. D., Y. J. Kaufman, W. P. Menzel, and D. Tanré (1992), Remote sensing of cloud, aerosol, and water vapor properties from the Moderate Resolution Imaging Spectrometer (MODIS), *IEEE Trans. Geosci. Remote Sens.*, *30*, 2–27.
- King, M. D., L. F. Radke, and P. V. Hobbs (1993), Optical properties of marine stratocumulus clouds modified by ships, *J. Geophys. Res.*, *98*, 2729–2739.
- King, M. D., W. P. Menzel, Y. J. Kaufman, D. Tanré, B. C. Gao, S. Platnick, S. A. Ackerman, L. A. Remer, R. Pincus, and P. A. Hubanks (2003), Cloud and aerosol properties, precipitable water, and profiles of temperature and humidity from MODIS, *IEEE Trans. Geosci. Remote Sens.*, *41*, 442–458.
- Kistler, R., et al. (2001), The NCEP-NCAR 50 year reanalysis: Monthly means CD-ROM and documentation, *Bull. Am. Meteorol. Soc.*, *82*, 247–267.
- Lebron, F. (1975), A comparison of weekend-weekday ozone and hydrocarbon concentrations in the Baltimore-Washington metropolitan area, *Atmos. Environ.*, *9*, 861–863.
- Lelieveld, J., et al. (2001), The Indian Ocean Experiment: Widespread air pollution from south and Southeast Asia, *Science*, *291*, 1031–1036.
- Linacre, E., and B. Geerts (2002), Estimating the annual mean screen temperature empirically, *Theor. Appl. Climatol.*, *71*, 43–61.
- Lonneman, W. A., S. L. Kocczynski, P. E. Darley, and F. D. Sutterfield (1974), Hydrocarbon composition of urban air pollution, *Environ. Sci. Technol.*, *8*, 229–236.
- Mace, G. G., Y. Zhang, S. Platnick, M. D. King, P. Minnis, and P. Yang (2005), Evaluation of cirrus cloud properties derived from MODIS radiances using cloud properties derived from ground-based data collected at the ARM SGP site, *J. Appl. Meteorol.*, in press.
- Marr, L. C., and R. A. Harley (2002a), Spectral analysis of weekday-weekend differences in ambient ozone, nitrogen oxide, and non-methane hydrocarbon time series in California, *Atmos. Environ.*, *36*, 2327–2335.
- Marr, L. C., and R. A. Harley (2002b), Modeling the effect of weekday-weekend differences in motor vehicle emissions on photochemical air pollution in central California, *Environ. Sci. Technol.*, *36*, 4099–4106.
- Oke, T. R. (1982), The energetic basis of the urban heat island, *Q. J. R. Meteorol. Soc.*, *108*, 1–24.
- Platnick, S., M. D. King, S. A. Ackerman, W. P. Menzel, B. A. Baum, J. C. Riédi, and R. A. Frey (2003), The MODIS cloud products: Algorithms and examples from Terra, *IEEE Trans. Geosci. Remote Sens.*, *41*, 459–473.
- Ramanathan, V., P. J. Crutzen, J. T. Kiehl, and D. Rosenfeld (2001), Aerosols, climate, and the hydrological cycle, *Science*, *294*, 2119–2124.
- Remer, L. A., and Y. J. Kaufman (1998), Dynamic aerosol model: Urban/industrial aerosol, *J. Geophys. Res.*, *103*, 13,859–13,872.
- Rissman, T. A., A. Nenes, and J. H. Seinfeld (2004), Chemical amplification (or dampening) of the Twomey effect: Conditions derived from droplet activation theory, *J. Atmos. Sci.*, *61*, 919–930.
- Rogers, R. R., and M. K. Yau (1989), *A Short Cloud Physics*, 3rd ed., 290 pp., Elsevier, New York.
- Rosenfeld, D. (2000), Suppression of rain and snow by urban and industrial air pollution, *Science*, *287*, 1793–1796.
- Schoeberl, M. R., and L. C. Sparling (1995), Trajectory modeling, in *Diagnostic Tools in Atmospheric Physics: Enrico Fermi CXVII*, edited by G. Fiocco and G. Visconti, pp. 289–305, Elsevier, New York.
- Shepherd, J. M., and S. J. Burian (2003), Detection of urban-induced rainfall anomalies in a major coastal city, *Earth Interactions*, *7*(4), doi:10.1175/10873562(2003)007.
- Shepherd, J. M., and M. Jin (2004), Linkages between the urban environment and Earth's climate system, *Eos Trans. AGU*, *85*, 227–228.
- Shepherd, J. M., H. Pierce, and A. J. Negri (2002), Rainfall modification by major urban areas: Observations from spaceborne rain radar on the TRMM satellite, *J. Appl. Meteorol.*, *41*, 689–701.
- Simpson, J., R. F. Adler, and G. R. North (1988), A proposed Tropical Rainfall Measuring Mission (TRMM) satellite, *Bull. Am. Meteorol. Soc.*, *69*, 278–295.
- Smirnov, A., B. N. Holben, T. F. Eck, O. Dubovik, and I. Slutsker (2000), Cloud screening and quality control algorithms for the AERONET data base, *Remote Sens. Environ.*, *73*, 337–349.
- Smirnov, A., B. N. Holben, T. F. Eck, I. Slutsker, B. Chatenet, and R. T. Pinker (2002), Diurnal variability of aerosol optical depth observed at AERONET (Aerosol Robotic Network) sites, *Geophys. Res. Lett.*, *29*(23), 2115, doi:10.1029/2002GL016305.
- Stull, R. B. (1988), *An Introduction to Boundary Layer Meteorology*, 670 pp., Springer, New York.
- Thompson, A. M., J. C. Witte, M. T. Freiman, N. A. Phahlane, and G. J. R. Coetzee (2002), Lusaka, Zambia, during SAFARI-2000: Convergence of local and imported ozone pollution, *Geophys. Res. Lett.*, *29*(20), 1976, doi:10.1029/2002GL015399.
- Tucker, C. J. (1979), Red and photographic infrared linear combinations for monitoring vegetation, *Remote Sens. Environ.*, *8*, 127–150.
- Twomey, S. (1977), The influence of pollution on the shortwave albedo of clouds, *J. Atmos. Sci.*, *34*, 1149–1152.

M. Jin, Department of Meteorology, University of Maryland, College Park, MD 20742, USA. (mj@atmos.umd.edu)

M. D. King, NASA Goddard Space Flight Center, Code 900, Greenbelt, MD 20771, USA.

J. M. Shepherd, NASA Goddard Space Flight Center, Code 912, Greenbelt, MD 20771, USA.